Available online at www.sciencedirect.com

ScienceDirect

Ceramics International 35 (2009) 2023–2028

CERAMICS INTERNATIONAL

www.elsevier.com/locate/ceramint

Development of electrochemical cell with layered composite of the Gd-doped ceria/electronic conductor system for generation of H_2–CO fuel through oxidation–reduction of CH_4–CO_2 mixed gases

Yoshihiro Hirata [a,*], Yujin Terasawa [b], Naoki Matsunaga [b], Soichiro Sameshima [a]

[a] Department of Advanced Nanostructured Materials Science and Technology, Kagoshima University, 1-21-40 Korimoto, Kagoshima 890-0065, Japan
[b] Department of Applied Chemistry and Chemical Engineering, Kagoshima University, 1-21-40 Korimoto, Kagoshima 890-0065, Japan

Received 10 September 2008; received in revised form 31 October 2008; accepted 9 November 2008
Available online 3 December 2008

Abstract

This paper shows the recent results on the development of layered composite promoting two types of electrochemical reactions (oxidation and reduction) in one cell. This cell consisted of porous Ni–Gd-doped (GDC) ceria cathode/thin porous GDC electrolyte (50 μm)/porous $SrRuO_3$–GDC anode. The external electric current was flowed in this cell at the electric field strength of 1.25 and 6.25 V/cm. The mixed gases of CH_4 (30–70%) and CO_2 (70–30%) were fed at the rate of 50 ml/min to the cell heated at 400–800 °C under the electric field. In the cathode, CO_2 was reduced to CO ($CO_2 + 2e^- \rightarrow CO + O^{2-}$) and the formed CO and O^{2-} ions were transported to the anode through the pores and surface and interior of grains of GDC film. On the other hand, CH_4 was oxidized in the anode to form CO and H_2 through the reaction with diffusing O^{2-} ions ($CH_4 + O^{2-} \rightarrow CO + 2H_2 + 2e^-$). As a result, H_2–CO mixed fuel was produced from the CH_4–CO_2 mixed gases ($CH_4 + CO_2 \rightarrow 2H_2 + 2CO$). This electrochemical reaction proceeded completely at 800 °C and no blockage of gases was measured for long time (>10 h). Only H_2–CO fuel was generated in the wide gas compositions of starting CH_4–CO_2 gases.

Keywords: A. Sintering; C. Chemical properties; D. CeO_2; E. Fuel cells

1. Introduction

Solid oxide fuel cell (SOFC) has many advantages such as high-energy conversion efficiency, clean product (H_2O), no loss of solid electrolyte and a variety of fuel gases. Rare earth-doped ceria (RDC) is a possible electrolyte for a low temperature SOFC at 600–800 °C because of its high oxide ion conductivity [1–4]. Reducing the operation temperature enhances the thermal stability of electrodes or interconnector and increases the lifetime of SOFC. Furthermore the transference number of oxide ion of RDC approaches unity by 10^{-15} Pa of oxygen partial pressure at 500 °C [5]. Recently biogas produced from excrement of domestic animals, which contains 60% of methane, 40% of carbon dioxide and a small amount of H_2S and NH_3 [6,7], has been evaluated as a SOFC fuel. The authors reported that the terminal voltage and electric power density of SOFC with Gd-doped ceria electrolyte (GDC) and porous Ni (30 vol%)–GDC anode were lower for biogas than for H_2 at 800 °C because of a high activation energy of thermal decomposition of CH_4 at a thin anode (thickness <100 μm) [8]. When the thickness of porous Ni (30 vol%)–Al_2O_3 compact is increased to 10 mm, pyrolysis of methane started at 400 °C. The thickness of the Ni-based anode is a key factor to operate SOFC using biogas. Barnett and co-workers reported a power density of 370 mW/cm^2 of SOFC using CH_4 fuel at 550 °C [9]. When carbon is deposited on the anode during the supply of methane, the electric power of SOFC decreases. Noble metals (Pt, Pd and Rh) are shown to suppress more the carbon deposition than Ni [10].

On the other hand, CH_4 is reformed with CO_2 to produce H_2 and CO which are used as fuels of SOFC ($CH_4 + CO_2 \rightarrow 2H_2 + 2CO$). This favorable reaction is expected to suppress the carbon deposition from methane. The hydrogen and carbon monoxide react with O^{2-} ion supplied from RDC electrolyte to form H_2O, CO_2 and electrons. The produced CO_2 may be again mixed with biogas

---

* Corresponding author. Tel.: +81 99 285 8325; fax: +81 99 257 4742.
E-mail address: hirata@apc.kagoshima-u.ac.jp (Y. Hirata).

0272-8842/$34.00 © 2008 Elsevier Ltd and Techna Group S.r.l. All rights reserved.
doi:10.1016/j.ceramint.2008.11.001

to make a closed system of $CO \rightarrow CO_2 \rightarrow CO$. That is, both methane and carbon dioxide of biogas can be used as fuels of SOFC. Some researchers use alkaline earth oxide or rare-earth oxide as a support material of Ni. These oxides adsorb CO_2 and accelerate the dissociation of CO_2 to CO and O. The formed O and CH_4 adsorbed on Ni react to form CO and H_2 [10]. Cui et al. [11] reported that reaction rate of reforming of CH_4 with CO_2 was dominated by the dissociation rate of CH_4 at low temperatures (<570 °C) and by rate of the reaction CH_x (adsorbed species derived from CH_4) and CO_2 at a high temperature (>630 °C). Shiratori et al. [12,13] investigated methane reforming activity for SOFC with NiO–Sc-stabilized zirconia (Sc-SZ) or $Ni_{0.9}Mg_{0.1}O$–ScSZ anode. The high performance of electrocatalyst was achieved by stabilizing the small Ni particles and by the formation of (Ni, Mg)O solid solution. In addition, humidified biogas was effective to prevent carbon deposition above 800 °C as compared with dry biogas. Kim et al. [14] reported the CO_2 reforming with CH_4 over Ni–YSZ (yttria-stabilized zirconia)–CeO_2 catalyst electrode in the electrochemical cell with YSZ electrolyte. Under open circuit condition, catalyst electrode was deactivated by coke deposition. However, CO and H_2 gases were produced at a high yield under short circuit condition. The coke formed was oxidized by oxide ions transported through dense YSZ electrolyte to anode catalyst. We also reported the basic information of reforming of CH_4 with CO_2 on Al_2O_3-supported 30 vol% of Ni catalyst at 400–700 °C to use biogas as a fuel of SOFC [15]. Carbon deposition occurred in the Ni–Al_2O_3 compact with large amount of Ni for electronic conduction and the blockage time became longer when the open porosity of the Ni–Al_2O_3 compact was increased.

To suppress the carbon deposition in the above catalytic reaction of CH_4–CO_2 mixed gases, this paper reports a new idea to produce a H_2–CO mixed fuel from a biogas using electrochemical cell. Carbon deposition was significantly suppressed during the electrochemical reaction of CH_4 and CO_2 gases at 800 °C. The produced H_2–CO fuel may be used as a fuel of SOFC. The electrochemical cell consists of porous Ni–GDC cathode/thin porous GDC electrolyte/porous $SrRuO_3$–GDC anode. CO_2 is reduced to CO in the cathode ($CO_2 + 2e^- \rightarrow CO + O^{2-}$) at the electric field strength of 1.25–6.25 V/cm. The formed CO and O^{2-} ions are transported to the anode through porous GDC film. CH_4 reacts with transported O^{2-} ions to form H_2 and CO gases. The yield of H_2 and CO gases was close to 100% at 800 °C.

2. Experimental procedure

2.1. Preparation of Ni–GDC cathode/GDC electrolyte/ $SrRuO_3$–GDC anode cell

The detailed preparation method of GDC powder was reported in our previous papers [1,2]. The oxalate solid solution, $(Ce_{0.8}Gd_{0.2})_2(C_2O_4)_3$, was produced by adding the mixed nitrate solution (0.2 M) of Ce and Gd into 0.4 M oxalic acid solution. The molar ratio of Ce to Gd was adjusted to 4/1. The produced coprecipitate was decomposed to GDC at 600 °C for 2 h. The GDC powder was milled with 3 mm diameter of alumina ball for 24 h. The milled GDC powder was immersed into a 1.4-M $Ni(NO_3)_2$ solution to make a cermet cathode with the volume ratio of Ni/GDC = 30/70 [16]. The 0.2-M mixed solution of $RuCl_3$ and $Sr(NO_3)_2$ with the molar ratio of Ru/Sr = 1/1 was added into 1 M NH_4OH solution and then freeze-dried. The $SrRuO_3$ powder was formed by heating the freeze-dried powder at 1000 °C for 2 h in air [17]. The 30 vol% solid suspension of $SrRuO_3$/GDC = 30/70 (vol%) at pH 10 was stirred for 6 h and then freeze-dried. The freeze-dried powder was heated at 600 °C for 1 h in air. GDC powder was consolidated to form a thin film on polyester sheet by doctor blade (DP-100, Tsugawa Seiki Seisakusho, Japan) at a transfer rate of 50 mm/min. The front and back blade clearance was controlled to be 150 and 80 μm, respectively. The formed film was left at room temperature for 24 h. The dried film was cut in a circle of 10 mm diameter. NiO–GDC powder, GDC film and $SrRuO_3$–GDC powder were layered, copressed uniaxially at 100 MPa for 1 min and then pressed isostatically at 294 MPa for 1 min. The green layered composite was sintered at 1200 °C for 2 h in air. The phases of the sintered $SrRuO_3$–GDC anode and Ni–GDC cathode were identified by X-ray diffraction (RINT 2200PCH/KG, Rigaku Co., Japan).

2.2. Electrochemical reaction of CH_4–CO_2 gases

Fig. 1 shows the scheme of electrochemical reaction apparatus. Pt wires were attached to the NiO–GDC cathode and $SrRuO_3$–GDC anode using Pt mesh and Pt paste. The NiO–GDC cathode/GDC electrolyte/$SrRuO_3$–GDC anode cell was set to an alumina holder and sealed at 900 °C for 10 min by using a glass O-ring. After cooling to 800 °C, H_2 gas was flowed into cathode at 50 ml/min for 24 h to reduce NiO to Ni ($NiO + H_2 \rightarrow Ni + H_2O$). After the reduction of NiO, the temperature was cooled down to 400 °C and 1 and 5 V of external voltage were applied by potentiostat (HA-501G, Hokuto Denko Co., Japan). The corresponding electric field strength and current density were 1.25 V/cm and 7.96×10^{-4} A/cm^2, and 6.25 V/cm and 3.96×10^{-3} A/cm^2 at 800 °C, respectively. The mixed gases of CH_4/CO_2 = 30/70, 40/60, 50/50, 60/40 and 70/30 (vol%) were fed into the cathode at 50 ml/min. The compositions of gases produced at 400–800 °C were analyzed by gas chromatography (GT 3800, Yanaco Co., Japan) with active carbon (60/80 mesh) using

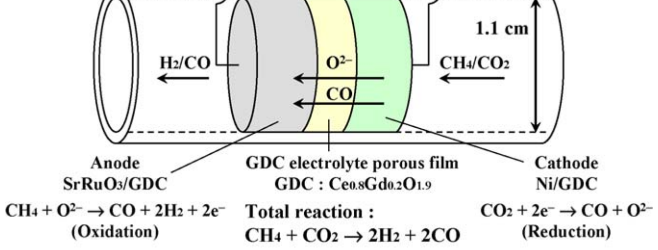

Fig. 1. Scheme of electrochemical reaction apparatus.

thermal conductivity detector at 100 °C. The outlet gas of 0.2 ml was injected into Ar carrier gas at 100 °C. The oxygen partial pressure of the outlet gas was monitored with yttria-stabilized zirconia oxygen gas sensor. The distribution of C element in the Ni–GDC cathode was measured by electron probe microanalyzer (EMX-SM7, Shimadzu Co., Japan).

3. Results and discussion

3.1. Properties of electrochemical cell

Fig. 2 shows the X-ray diffraction patterns of $SrRuO_3$–GDC anode heated at (a) 600 °C, (b) 700 °C and (c) 800 °C for 1 h in air. The diffraction peaks heated at 600 °C were identified as GDC, $SrRuO_3$, $SrCl_2$ and RuO_2. $SrCl_2$ was formed by the reaction between $RuCl_3$ and SrO in air ($RuCl_3 + SrO + 1/2O_2 \rightarrow RuO_2 + SrCl_2 + 1/2Cl_2$). At 700–800 °C, the thermal decomposition of $SrCl_2$ proceeded and the formation of $SrRuO_3$ from SrO and RuO_2 was accelerated. No chemical reaction was suggested between $SrRuO_3$ and GDC [17]. Similarly, Ni and GDC coexisted in the cathode after the reduction of NiO with H_2 gas. The $SrRuO_3$–GDC anode and Ni–GDC cathode contained 35.9 and 42.6% of open pores and 12.6 and 7.8% of closed pores, respectively. Fig. 3 shows the GDC film of 50 μm thickness sintered at 1200 °C in air. The film has a porous structure to transport the CH_4–CO_2 mixed gases. When the sintering temperature was increased to 1400 °C, a dense microstructure without pores was formed [18]. The dense microstructure is not suitable to the purpose of this study.

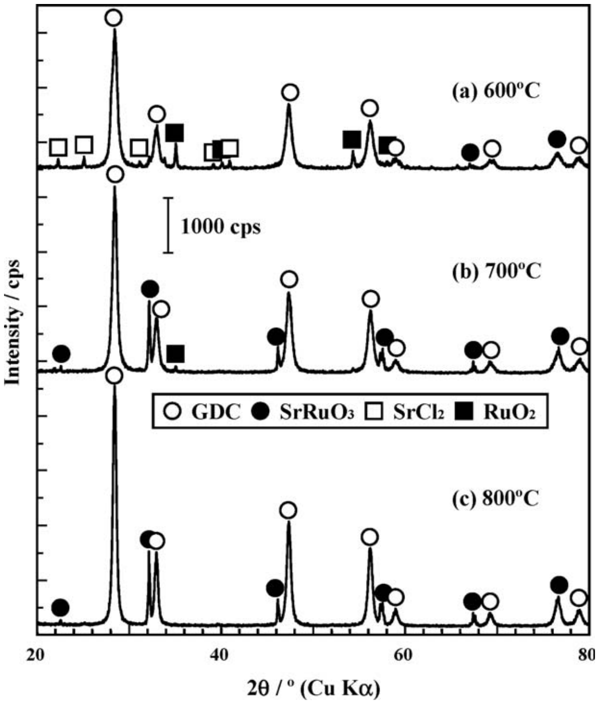

Fig. 2. X-ray diffraction patterns of $SrRuO_3$–GDC anode after heating of the mixtures of GDC, $Sr(NO_3)_2$ and $RuCl_3$ at (a) 600 °C, (b) 700 °C and (c) 800 °C for 1 h in air.

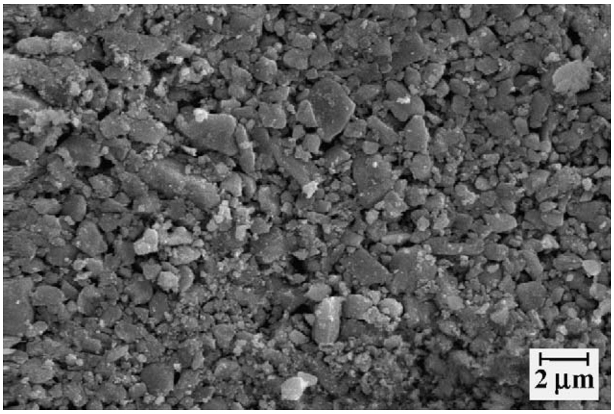

Fig. 3. Surface structure of the GDC electrolyte film sintered at 1200 °C for 2 h in air.

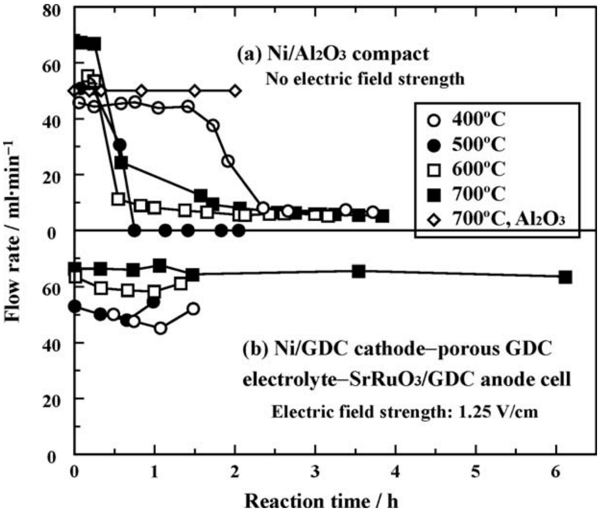

Fig. 4. Time dependence of flow rate of outlet gas through Ni–Al_2O_3 compact (a) and electrochemical cell operated at 1.25 V/cm of electric field strength (b) at 400–700 °C.

Fig. 4 shows the flow rates of outlet gases through Ni–Al_2O_3 compact (a) and the electrochemical cell at 1.25 V/cm of electric field strength (b). CH_4 of 25 ml/min and CO_2 of 25 ml/min were mixed and fed into the Ni–Al_2O_3 compact or the electrochemical cell. When the mixed gases were flowed into an Al_2O_3 compact without Ni (Fig. 4(a)), no change of the flow rate of the outlet gas was measured, suggesting no reaction between CH_4 and CO_2 at 700 °C [15]. Pyrolysis of CH_4 in a SiO_2–Al_2O_3 tube occurred above 900 °C [19]. On the other hand, the flow rate of the outlet gas through the Ni–Al_2O_3 compact decreased after 0.5 h of reaction time. The blockage of gas flow occurred at 2.35, 0.75, 0.55 and 1.72 h at 400, 500, 600 and 700 °C, respectively. These results were associated with the carbon deposition in the Ni–Al_2O_3 compact [15]. When the Ni–GDC cathode/GDC electrolyte/$SrRuO_3$–GDC anode cell was operated at 1.25 V/cm, no decrease of the flow rate of the outlet gas was measured at 400–700 °C. The cumulative reaction time at 400–700 °C was 11 h. The stable flow rate is related to the electrochemical reactions expressed by Eqs. (1) and (2) at cathode and anode, respectively:

$$CO_2\,(g) + 2e^- \rightarrow CO\,(g) + O^{2-} \quad (1)$$

$$CH_4\,(g) + O^{2-} \rightarrow CO\,(g) + 2H_2\,(g) + 2e^- \quad (2)$$

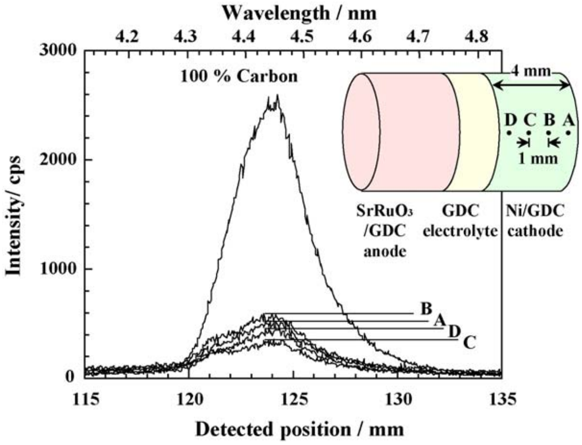

Fig. 5. Content of carbon deposited in Ni–GDC cathode operated at 1.25 V/cm of electric field strength at 400–700 °C for 11 h. The wavelength of X-ray detected by EPMA is proportional to the detected position. The wavelength of 4.45 nm corresponds to the X-ray from carbon.

The total reaction is expressed by Eq. (3):

$$CH_4\,(g) + CO_2\,(g) \rightarrow 2H_2\,(g) + 2CO\,(g) \quad (3)$$

Fig. 5 shows the content of carbon distributed in Ni–GDC cathode operated at 1.25 V/cm of electric field strength at 400–700 °C for 11 h. Four points of (A)–(D) with 1 mm interval were analyzed by EPMA. Carbon was homogeneously deposited in the cathode. Compared with reference carbon of purity 100%, the deposited carbon content was in the range of 13–18%. As seen in Fig. 4(b), blockage by carbon deposition was not observed in this experiment. That is, the electrochemical cell used suppresses the formation of carbon and promotes the reforming of CH_4 with CO_2 (Eq. (3)).

3.2. Formation of H_2–CO fuel

Fig. 6 shows fractions of CH_4, CO_2, H_2 and CO gases through the electrochemical cell operated at 1.25 V/cm. The 50 vol% CH_4–50 vol% CO_2 mixed gases decomposed to H_2 and CO. The gas fraction at each temperature was independent of the reaction time. The amounts of remaining CH_4 and CO_2 were approximately 10 and 13% at 700 °C, respectively.

Fig. 7 shows the relationship between molar ratio of CH_4–CO_2 of inlet gas and fractions of outlet gas through the cell operated at (a) 1.25 V/cm and (b) 6.25 V/cm at 800 °C (corresponding current density was 7.96×10^{-4} and 3.96×10^{-3} A/cm^2, respectively). The CH_4–CO_2 mixed gases were almost changed to H_2 and CO at 1.25 V/cm in the wide inlet gas compositions. The fraction of H_2 gas increased at a higher fraction of CH_4. Opposite tendency was measured for CO formation. A similar result was observed at 6.25 V/cm of electric field strength (Fig. 7(b)). However, when the mixed ratio of CH_4–CO_2 was less 1, a small amount of CO_2 remained in the outlet gas. This result is discussed latterly and indicates that the reaction mechanism between CH_4 and CO_2 gases depends on the applied electric field strength. The quantity of electricity for the amounts of H_2 and CO produced is 10^4 times as large as the quantity of electricity flowed by the external circuit. This result indicates that (1) the reforming of CH_4–CO_2 mixed gases proceeds over the electrodes through catalytic reaction and (2) the electrochemical efficiency of the quantity of electricity flowed may reach 100% because of the high ratio between the calculated and measured quantities of electricity.

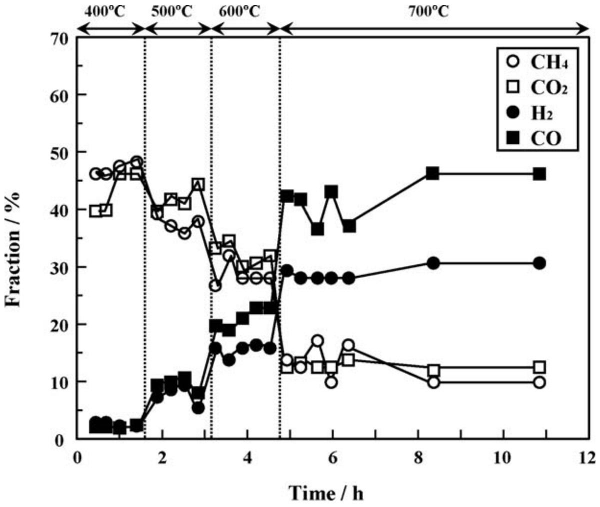

Fig. 6. Fractions of CH_4, CO_2, H_2 and CO through electrochemical cell operated at 1.25 V/cm. The 50 vol% CH_4–50 vol% CO_2 mixed gases decomposed to H_2 and CO gases.

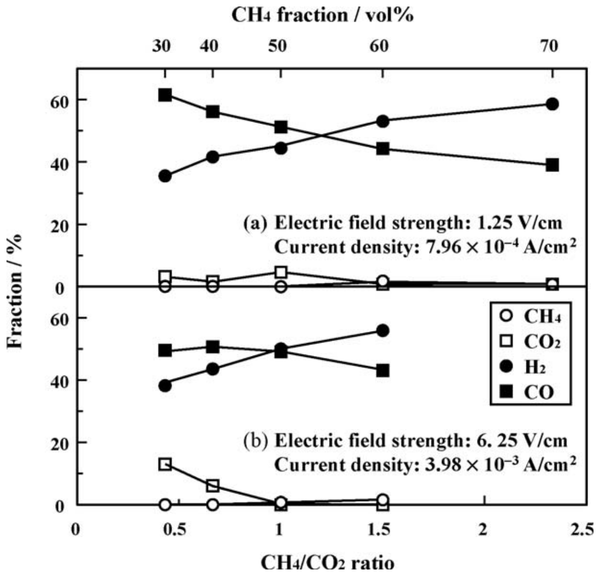

Fig. 7. Relationship between molar ratio of CH_4–CO_2 of inlet gas and fraction of outlet gas through electrochemical cell operated at (a) 1.25 V/cm and (b) 6.25 V/cm at 800 °C.

Fig. 8 shows the molar ratio of H_2 to CO of outlet gas as a function of the reaction temperature for the inlet gas of CH_4–CO_2 = 1. When the CH_4–CO_2 gases were fed into the Ni–Al_2O_3 compact, the H_2–CO ratio was in the range of 2–3. This result and the blockage in Fig. 4(a) are explained by the carbon deposition (Eq. (4) or (5)):

$$CH_4\,(g) \rightarrow C\,(s) + 2H_2\,(g) \quad (4)$$

$$2CO\,(g) \rightarrow C\,(s) + CO_2\,(g) \quad (5)$$

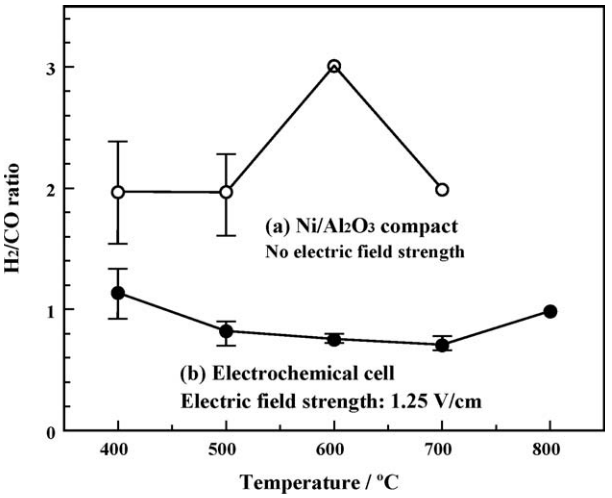

Fig. 8. Molar ratio of H_2 to CO of outlet gas as a function of reaction temperature.

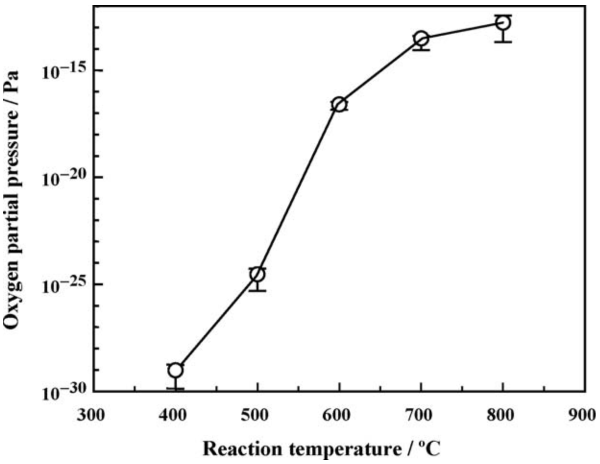

Fig. 9. Oxygen partial pressure of outlet gas through the cell.

The CO formed by Eq. (3) may be decomposed to C and CO_2 by Eq. (5) at 400–600 °C [15]. On the other hand, the molar ratio of H_2–CO was close to 1 for the cell operated at 1.25 V/cm in the wide temperature range. This result indicates that the reforming of CH_4 with CO_2 expressed by Eq. (3) is the dominant reaction in the electrochemical cell.

Fig. 9 shows the oxygen partial pressure of outlet gas through the cell for the inlet gas of 50 vol% CH_4–50 vol% CO_2. The measured oxygen pressure was 10^{-29} to 10^{-12} Pa at 400–700 °C. This small value of oxygen pressure denies the direct reaction of CH_4 and O_2 in the mixed gases to form CO and H_2.

Fig. 10 shows the relationship between the molar ratio of CH_4–CO_2 gases (A) used to electrochemical reaction and the molar ratio of H_2–CO gases formed (B). When the following parallel reactions proceed at a same time, B value is equal to $(3A - 1)/(A + 1)$:

$$CH_4\,(g) + CO_2\,(g) \rightarrow 2H_2\,(g) + 2CO\,(g) \tag{3}$$

$$CH_4\,(g) + 3CO_2\,(g) \rightarrow 4CO\,(g) + 2H_2O\,(g) \tag{6}$$

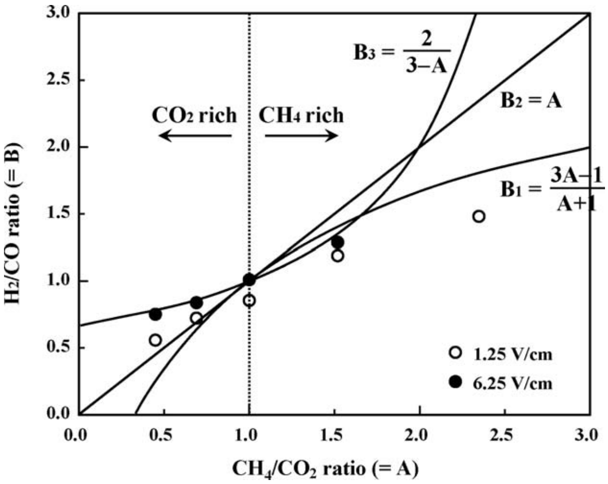

Fig. 10. Relationship between molar ratio of CH_4–CO_2 gases (A) used to chemical reaction and molar ratio of H_2–CO gases formed (B). The measured B values were plotted against the mixed ratio of CH_4–CO_2 of inlet gas at 800 °C.

The cathode and anode reactions for Eq. (6) are expressed by Eqs. (7) and (8), respectively:

$$3CO_2 + 6e^- \rightarrow 3CO + 3O^{2-} \tag{7}$$

$$CH_4 + 3O^{2-} \rightarrow CO + 2H_2O + 6e^- \tag{8}$$

When Eqs. (3) and (4) proceed at a same time, B value is equal to A:

$$CH_4\,(g) + CO_2\,(g) \rightarrow 2H_2\,(g) + 2CO\,(g) \tag{3}$$

$$CH_4\,(g) \rightarrow C\,(s) + 2H_2\,(g) \tag{4}$$

On the other hand, the parallel reactions of Eqs. (3) and (9) lead to the relation of $B = 2/(3 - A)$:

$$CH_4\,(g) + CO_2\,(g) \rightarrow 2H_2\,(g) + 2CO\,(g) \tag{3}$$

$$3CH_4\,(g) + CO_2\,(g) \rightarrow 2H_2\,(g) + 2CH_3CHO\,(g) \tag{9}$$

Acetaldehyde (CH_3CHO) may be formed by the chemical reaction of CH_4 and CO electrochemically formed through Eq. (1):

$$CH_4\,(g) + CO\,(g) \rightarrow CH_3CHO\,(g) \tag{10}$$

In Fig. 10, the measured B values were plotted against the mixed ratio of CH_4–CO_2 of inlet gas at 800 °C. The measured B value at 6.25 V/cm of electric field strength was well fitted by B_3 in Fig. 10. The B value at 1.25 V/cm was close to B_2 at $A < 1$ and B_1 at $A > 1$. In the range of $A < 1$, the deposited C may react with the excess CO_2 to form CO. The above good agreement of A–B relation between the experimental results and the proposed electrochemical reactions suggests that the dominant electrochemical reactions depend on the applied voltage and the mixing ratio of CH_4–CO_2. Further experiment will be measured to analyze the reaction mechanism.

Fig. 11 shows X-ray diffraction patterns of (a) Ni–GDC cathode and (b) $SrRuO_3$–GDC anode after the reforming of CH_4–CO_2 mixed gases at 600–800 °C for 11 h. In the Ni–GDC

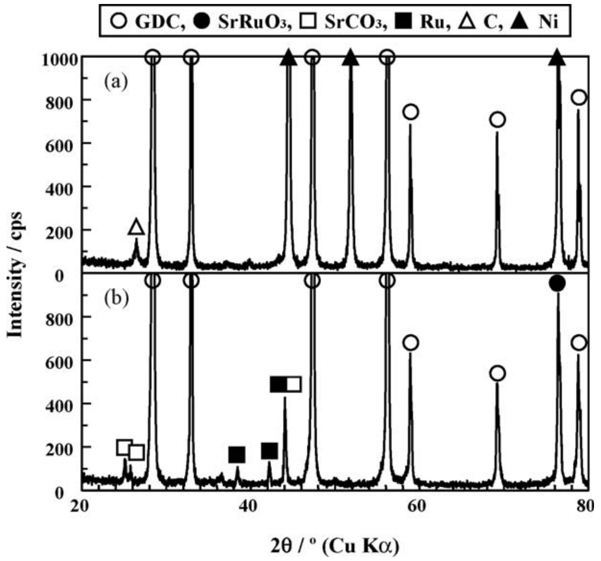

Fig. 11. X-ray diffraction patterns of (a) Ni–GDC cathode and (b) $SrRuO_3$–GDC anode after reforming of CH_4 and CO_2 mixed gases at 600–800 °C for 11 h.

cathode, GDC, Ni and C were identified (Fig. 11(a)). This result indicates that (1) Ni and GDC are stable in the atmosphere of low oxygen pressure (Fig. 9) and (2) a part of CH_4 decomposed to C and H_2 over the cathode. On the other hand, in the $SrRuO_3$–GDC anode, GDC, Ru and $SrCO_3$ were identified (Fig. 11(b)). This result indicates that $SrRuO_3$ decomposed to Ru and SrO in the low oxygen pressure ($SrRuO_3 \rightarrow SrO + Ru + O_2$) and the produced SrO reacted with CO_2 to form $SrCO_3$ ($SrO + CO_2 \rightarrow SrCO_3$). However, the electronic conduction of the anode is caused by Ru metal formed.

4. Conclusions

Electrochemical reforming of CH_4 with CO_2 in the wide composition ratios of CH_4–CO_2 proceeded through the Ni–GDC cathode/GDC porous electrolyte/$SrRuO_3$–GDC anode cell operated at 1.25–6.25 V/cm of electric field strength to form H_2 and CO at 400–800 °C. This cell suppressed the carbon deposition accompanied by the decomposition of CH_4 and no blockage was measured for the long time (>10 h). The H_2–CO ratio of produced fuel was controlled by the applied voltage of cell and the starting mixing ratio of CH_4–CO_2. The $SrRuO_3$ in the anode decomposed to Ru and $SrCO_3$ in the CH_4–CO_2 mixed gas.

References

[1] K. Higashi, K. Sonoda, H. Ono, S. Sameshima, Y. Hirata, Synthesis and sintering of rare-earth-doped ceria powder by the oxalate coprecipitation method, J. Mater. Res. 14 (1999) 957–967.

[2] K. Higashi, K. Sonoda, H. Ono, S. Sameshima, Y. Hirata, Characterization of rare earth-doped ceria powders derived from oxalate coprecipitate, Key Eng. Mater. 159 (160) (1999) 25–30.

[3] S. Sameshima, H. Ono, K. Higashi, K. Sonoda, Y. Hirata, Y. Ikuma, Electrical conductivity and diffusion of oxygen ions in rare-earth-doped ceria, J. Ceram. Soc., Jpn. 108 (2000) 1060–1066.

[4] Y. Hirata, S. Yokomine, S. Sameshima, T. Shimonosono, S. Kishi, H. Fukudome, Electrochemical properties of solid oxide fuel cell with Sm-doped ceria electrolyte and cermet electrodes, J. Ceram. Soc., Jpn. 113 (2005) 597–604.

[5] T. Shimonosono, Y. Hirata, S. Sameshima, T. Horita, Electronic conductivity of La-doped ceria ceramics, J. Am. Ceram. Soc. 88 (2005) 2114–2120.

[6] Y. Lu, L. Schaefer, A solid oxide fuel cell system fed with hydrogen sulfide and natural gas, J. Power Sources 135 (2004) 184–191.

[7] M. Nagamori, Y. Hirata, S. Sameshima, Influence of hydrogen sulfide in fuel on electric power of solid oxide fuel cell, Mater. Sci. Forum 544 (545) (2007) 985–988.

[8] H. Ohshige, Y. Hirata, S. Sameshima, Electrochemical properties of solid oxide fuel cell using biogas, Adv. Ceram. Proc. Int. 3 (2006) 1–4.

[9] E.P. Murray, T. Tsai, S.A. Barnett, A direct-methane fuel cell with a ceria-based anode, Nature 400 (1999) 649–651.

[10] K. Tomoshige, K. Fujimoto, Catalytic performance and analysis of carbon deposition in the production of synthesis gas by methane reforming with carbon dioxide—development of NiO–MgO solid solution catalysis, J. Jpn. Petrol. Inst. 44 (2001) 65–79 (in Japanese).

[11] Y. Cui, H. Zhang, H. Xu, W. Li, Kinetic study of the catalytic reforming of CH_4 with CO_2 to syngas over Ni/α–Al_2O_3 catalyst: the effect of temperature on the reforming mechanism, Appl. Catal. A: Gen. 318 (2007) 79–88.

[12] Y. Shiratori, Y. Teraoka, K. Sasaki, $Ni_{1-x-y}Mg_xAl_yO$–ScSZ anodes for solid oxide fuel cells, Solid State Ionics 177 (2006) 1371–1380.

[13] Y. Shiratori, K. Sasaki, NiO–ScSZ and $Ni_{0.9}Mg_{0.1}O$–ScSZ-based anodes under internal dry reforming of simulated biogas mixtures, J. Power Sources 180 (2008) 738–741.

[14] T. Kim, S. Moon, S.-I. Hong, Internal carbon dioxide reforming by methane over Ni–YSZ–CeO_2 catalyst electrode in electrochemical cell, Appl. Catal. A: Gen. 224 (2002) 111–120.

[15] S. Sameshima, Y. Hirata, J. Sato, N. Matsunaga, Synthesis of hydrogen and carbon monoxide from methane and carbon dioxide over Ni–Al_2O_3 catalyst, J. Ceram. Soc., Jpn. 116 (2008) 374–379.

[16] Y. Okawa, Y. Hirata, Sinterability, microstructures and electrical properties of Ni/Sm-doped ceria cermet processed with nanometer-sized particles, J. Eur. Ceram. Soc. 25 (2005) 473–480.

[17] T. Shimonosono, G. Hiramatsu, Y. Hirata, S. Sameshima, N. Matsunaga, T. Doi, T. Horita, Electrochemical properties of cathode for solid oxide fuel cell with Gd-doped ceria electrolyte, Adv. Mater. Res. 26 (28) (2007) 275–278.

[18] M. Nagamori, T. Shimonosono, S. Sameshima, Y. Hirata, N. Matsunaga, Y. Sakka, Densification and cell performance of Gd-doped ceria (GDC) electrolyte/NiO–GDC anode laminates, J. Am. Ceram. Soc., 92, in press.

[19] S. Sameshima, Y. Hirata, K. Hamasaki, H. Ohshige, N. Matsunaga, Synthesis of hydrogen–carbon monoxide fuel from methane–carbon dioxide mixed gases, J. Ceram. Soc., Jpn., submitted for publication.